

# A hybrid NN-FE approach to adjust blank holder gap over punch stroke in deep drawing process

Abbas Hosseini · Mehran Kadkhodayan

Received: 19 July 2012 / Accepted: 5 November 2013 / Published online: 26 November 2013  
© Springer-Verlag London 2013

**Abstract** In deep drawing process, the blank holder plays a key role in adjustment of metal flow into the die cavity. Moreover, the quality of drawn parts is extremely affected by this flow. There are two methods of treating the blank holder in deep drawing and its simulation. One is blank holder force (BHF) and the other is blank holder gap (BHG), defined as the fixed distance between the blank holder and the die surface. In previous studies, a large number of experimental techniques have been used to study BHF; however, the amount of theoretical and numerical simulation work to study BHG is insufficient. In the present study, the concept of BHG profile, i.e., variation of BHG over punch stroke is introduced and it is shown that a properly selected BHG profile can improve the section thickness of formed part and result in the drawing of deeper parts. Here, two methods for the optimization of BHG profile are devised, i.e., the local optimization and the global optimization methods. In the first approach, the best BHG in each punch step is determined and finally, the local optimized BHG profile is achieved. In the second method, however, the empirical model for the prediction of final minimum section thickness in terms of BHG profile is obtained using design of experiments and neural networks. In the next stage, the proposed model is implanted into a simulated annealing optimization procedure to identify a proper BHG profile that can produce the desired blank thickness. Afterward, the BHG profile approach is applied to a variety of initial thicknesses, blank diameters, and materials

in order to examine the robustness of method. In this paper, ABAQUS finite element package is used to gather finite element (FE) data and several experiments are performed to verify the FE results.

**Keywords** Deep drawing process · Blank holder gap profile · Optimization procedure · Artificial neural network · Simulated annealing algorithm

## 1 Introduction

Sheet metal forming is one of the most common manufacturing processes to plastically deform a material into a desired shape [1]. In sheet metal forming, the production of thinner products has become important because of recent increasing demands for the miniaturization of electrical devices by introducing compact and lightweight components, particularly in electrical industries [2]. In deep drawing, the quality of the formed part is affected by the amount of metal drawn into the die cavity [3]. It is known that drawability significantly decreases with decreasing blank thickness [2].

In sheet stamping operation, wrinkling normally occurs at the flange and is generated by excessive compressive stresses that cause the sheet to buckle locally. On the other hand, fracture or necking occurs in a drawn part which is under excessive tensile stresses. Wrinkling and tearing rupture thus define the deep drawing process limits.

For a given problem, many variables affect the failure of a stamping operation. These include material properties, die design, and process parameters such as friction conditions, the drawing ratio as well as the blank holder force (BHF)/gap (BHG). It is reported in the literature that the careful control of these parameters can delay the failure of the part. Among these process and design variables, the BHF [3] and BHG

A. Hosseini (✉) · M. Kadkhodayan  
Department of Mechanical Engineering, Ferdowsi University of  
Mashhad, Mashhad, Iran  
e-mail: abb.hosseini@um.ac.ir

M. Kadkhodayan  
e-mail: kadkhoda@um.ac.ir

[4] can greatly influence the growth and development of part defects.

As earlier mentioned, there are two methods of treating the blank holder in deep drawing and its simulation. One is BHF and the other is BHG, defined as the fixed distance between the blank holder and the die surface [5]. In a typical sheet stamping operation, a blank of sheet is held between a holder and a die. In the first step, a blank holder force is applied to provide a restraining force to the sheet through the frictional force from the holder interface and then, the punch moves down to draw material into the die cavity and plastically deform the material into the desired shape [1].

In conventional deep drawing processes, the blank holder force applied to the sheet blank is constant during the process [3], whereas the state of stress in the deforming material changes significantly. As a consequence, the process conditions that produce wrinkling and fracture also change.

A large number of experimental techniques have been used to study BHF. However, the amount of theoretical and numerical simulation work to study BHG is insufficient [4]. Although some studies [5] have involved an analytical model, the BHG is not yet fully understood. Hence, a brief review to the progress of BHF and BHG accompanied with the current technologies are of utmost importance.

Since the state of stress in the deforming material changes noticeably, it is wise to change the blank holder force during deep drawing process. This concept has been the building block of previous research works into variable blank holder systems. In the literature, there are several methods in order to determine a suitable blank holder force profile, i.e., variation of BHF over punch stroke. A good variable BHF profile, for example, was determined by conducting time-consuming finite element (FE) simulations or experimental trials [6].

An analytical method to predict the BHF profile for simple part geometries was proposed by Seibel. However, acceptable agreements with experimental observations have not been obtained for most analytically predicted BHF profiles [7].

Nowadays, closed-loop-controlled FE simulation is one of the most efficient methods to predict variable BHF. In this method, the forming process is simulated using a finite element (FE) software, and appropriate BHF levels are determined based on the process parameters, i.e., wrinkling amplitude, section thickness of the formed part and so on, obtained at any given time step. Therefore, the BHF is continuously regulated over the punch stroke and finally, a desirable BHF profile is achieved.

Cao and Boyce [1] optimized deep drawing process of a conical cup using a similar method to provide a variable BHF. In their research, two of the primary in process failure modes of sheet metal was examined, i.e., wrinkling and tearing. To detect the failure modes, major principal strains, and

amplitudes of wrinkles occurring at the die radius were used as state variables for adjusting BHF.

Thomas reported [6] that the prediction of optimal process parameters will focus primarily on determining the optimum time and spatial variation of BHF given a particular geometry. Then, he proposed a closed-loop-controlled system based on FE analysis to improve the drawability of a round cup and rectangular pan. In his study, several important parameters including the punch load, the amplitudes of wrinkles, and the maximum strains and stresses were considered as process parameters.

In Sheng's study [3], a feedback-controlled strategy, which is similar to the closed-loop strategy used in [8, 9], was developed and integrated into PAM-STAMP, a commercial FEM code. Although the control algorithm employed in Sheng's study was similar to the Cao and Boyce's work [9], the in process failure modes of sheet metal were different. As earlier mentioned, major principal strains and flange wrinkle amplitudes were considered as state variables in Cao and Boyce's method; however, Sheng's control algorithm utilizes maximum part thinning, flange wrinkle, as well as side wall wrinkle amplitudes calculated at every simulation time step.

As aforementioned, a large number of attempts have been made to study BHF, while the amount of theoretical and numerical work to study BHG is insufficient. Hence, most of works related to BHG are going to be presented here.

Huaibao et al. [5] provided the nature of stamping and two advantages of stamping simulation with a constant blank holder gap. In stamping simulation, there are two advantages in using the BHG method. It can simulate the binder wrap and the followed drawing process contiguously without any artificial interface, and it can verify the rationality of die design effectively. The effect of blank holder gap on deep drawing of square cups with ETIAL-8 sheets was studied by Gavas and Izciler [10]. In their work, different constant blank holder gaps ranging from 1 to 1.8 mm for 1 mm aluminum sheets were used in the experiments. The experimental implementation showed that a reasonable value of blank holder gap has a great effect on the forming quality of the final part. Finally, a suitable constant blank holder gap for deep drawing of square cup for given tooling and material was proposed. Chen et al. [4] reported that the wrinkling in the flange region of the blank turn larger with the increase of the blank holder gap and the reaction force to the blank holder increases first and decreases gradually with the variety of the stiffness of the sheet metal. Then, an optimum constant BHG was recommended at given process parameters.

The influence of controlling blank holder motion by a newly proposed algorithm on deep drawability was investigated by Yagami et al. for a circular cup of a thin sheet metal from the perspective of wrinkle behavior as well as the fracture limit [2]. In their research, the blank holder force was

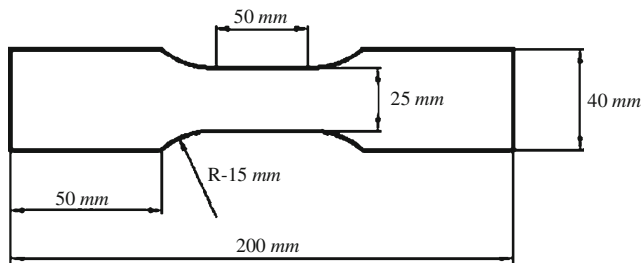


**Fig. 1** Tensile test specimens

taken extremely low by temporarily allowing wrinkling to improve the drawability of thin blanks.

In the literature, a variety of studies have been conducted in order to make use of artificial neural networks (ANN) in sheet metal-forming processes. Singh and Kumar [11] employed an artificial neural network to predict the distribution of section thickness in hydromechanical deep drawing operation and they utilized a model with feed-forward back-propagation neural network. Thenceforth, the model was applied to new data in order to predict the thickness strains in hydromechanical deep drawing process. Finally, they reported that a more desirable drawability with acceptable uniformity in thickness distribution can be achieved by this process in comparison with conventional deep drawing operation.

Cao et al. [12] proposed an exceptional ability of a neural network along with a stepped blank holder force trajectory to control spring-back angle and maximum principal strain in a channel forming process. Satoshi et al. [13] developed a new approach to optimize a variable blank holder force trajectory by using sequential approximate optimization with RBF network which is one of the artificial neural networks. Chamekh et al. [14] reported that the transformation of the sheet into a product without failure and excess of material in a deep drawing operation means that the initial blanks should be correctly designed. Afterward, they built a metamodel based on artificial neural networks which was coupled with an optimization procedure for the prediction of an optimized initial blank shape in a rectangular cup deep drawing process.

By reviewing the researches in literature, it was discovered that the blank holder gap was considered as a fixed distance between the die and blank holder and the optimum constant distance during the process was determined, whereas the state of stress in the deforming material was changed significantly. Thereupon, it is evident that determination of a variable blank holder gap during deep drawing process by considering the state of stress can be considered as an important need. It should be noted that although the blank holder gap was not

constant in Yagami's work, the state of stress and blank thickness have not been desirably controlled during the process. Moreover, loading history as one of the most important parameters in forming processes was ignored.

In the present study, the concept of blank holder gap profile is introduced, and then two different methods are employed in order to determine the optimum blank holder gap profile, the local and the global optimization methods. The first method is based on the selection of corresponding BHG to the best thickness of the drawn part in each punch step. In other words, four FE simulations with different BHGs are performed in each punch step and then, BHG corresponds to desirable thickness of the formed part is chosen.

As reported above, there is no major study in previous researches in order to model and optimize blank holder gap over punch stroke using artificial neural networks and accordingly, concentration upon this approach can be extremely arousing. In this study, the global optimization procedure utilizes artificial neural networks and simulated annealing algorithm to find the global optimized BHG profile. In this approach, all effective parameters in deep drawing process including the state of stress, loading history, and thinning are indirectly considered and then, a global optimized BHG profile is achieved.

To validate the FE results, two sheet blanks of aluminum 1100 with diameters of 120 and 130 mm and thickness of 0.49 mm were drawn using a constant blank holder force. Thenceforth, a Cyclone Digitizer-series 2 determined the final minimum thickness in each deformed part. Next, the final minimum thickness and the diagram of punch force–punch displacement were compared with FE simulation results and good agreements were revealed. Considering FE and experimental results, the accuracy of FE simulation parameters was proved and afterwards, FE model was employed in lieu of experiments to gather data.

In the local optimization method, FE simulations are used in each punch step and then, the optimized BHG profile is obtained. Furthermore, the global optimization method utilizes the finite element data to relate the blank holder gaps in different steps, i.e., BHG profile, to final minimum thickness through developing a model in neural networks. In the next stage, the proposed model is implanted into a simulated annealing (SA) optimization procedure to identify a proper BHG profile that can produce the desired blank thickness and LDR.

To investigate the generalization of BHG profile approach, this concept has been applied to a variety of initial thicknesses, blank diameters, and materials. Finally, several experiments

**Table 1** Chemical composition and mechanical properties of aluminum 1100

Nuance	Al %	Cu %	Fe %	Mg %	Si %	Ti %	Mn %	Zn %	$\sigma_y$ MPa	$\sigma_{UTS}$ MPa	Young's module GPa
Al 1100	99	0.05	0.42	0.03	0.32	0.03	0.05	0.10	27	95	64

are performed by optimum BHG profiles and the results are compared with those of constant blank holder force method. The thickness distributions in the deformed parts by optimized BHG profiles are improved in comparison with those of obtained by constant blank holder force approach.

## 2 Material characteristics

The annealed aluminum alloy was supplied in sheet form 0.49 mm thick and cut into specimens of the form and the final dimensions shown in Fig. 1. The chemical composition and mechanical properties of this material are presented in Table 1. In this paper, a complete experimental characterization was carried out in order to identify the material behavior. A tensile test machine with maximum test force 250 kN was employed to carry out uniaxial tensile test. In this study, all tensile tests were performed at 0°, 45°, and 90° to the rolling direction (RD) for the investigation of sheet metal anisotropy. Moreover, two extensometers were utilized to measure the longitudinal and transverse strains. Three tests were performed each time to check the reproducibility of the experiments.

### 2.1 Tensile tests

The tensile test specimens were cut on the initial cold rolled sheets at different orientations to the RD (0°, 45°, and 90°). The speed of testing was defined in terms of the rate of separation of the two heads of the testing machine and corresponds to a strain rate of 0.002 ( $\frac{1}{s}$ ). Logarithmic strain and stress were used throughout the paper to plot stress–strain data, see Fig. 2.

In this research, the plastic anisotropy of the plate was assessed by Lankford's coefficients,  $r_\theta = \frac{d\varepsilon_x^p}{d\varepsilon_z^p}$ , where  $\varepsilon_x$ ,  $\varepsilon_y$ ,

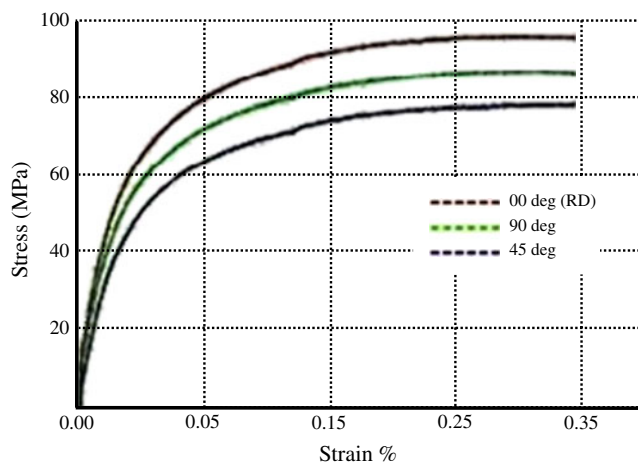


**Fig. 2** Stress–strain curves at different degrees to the rolling direction

**Table 2**  $R$  values in different directions

Nuance	$r_0$	$r_{45}$	$r_{90}$
Al 1100	0.69079	1.06005	0.65393

and  $\varepsilon_z$  are the strains in the length, width, and thickness directions obtained in a tensile test respectively.  $R$  values in different directions are tabulated in Table 2. Considering the material properties and experimental conditions, preliminary experiments show that the blanks with diameters of equal and less than 125 mm are drawn without failure. Hence, the primary blank diameter in the current experiments was chosen as 120 mm.

### 2.2 Coefficient of friction

One of the most important needs in finite element modeling of deep drawing process is to determine the coefficients of friction between sheet blank and different tools. It is reported in the literature that the coefficient of friction in deep drawing process is not same in various regions and several tests are needed to extract these values. Basic strip-pull and draw-bend tests, for example, must be performed in order to specify the coefficients of friction in the flange area and punch/die radius, respectively.

In most researches into FE simulation of deep drawing process, a constant coefficient of friction is assumed in different areas since incorporation of all the regions is not possible with Coloumb's friction model which is widely used in FE simulations. In the literature [3], a constant value for the friction coefficient of aluminum alloy 1100 was derived by performing several experiments. In the present study, the same material is employed in the experimental procedures; nevertheless, some tests were carried out to investigate the consistency of the previous results with the present conditions.

To consider the accuracy of results presented in the literature, a basic strip-pull test was performed using a force-gauge of resolution 0.01 N. The coefficients of friction extracted from the tests revealed acceptable agreements with those obtained in [3].



**Fig. 3** Hydraulic press employed in the experiments

**Table 3** Boundary conditions applied to the sheet metal mesh

Direction	Node at the center of the mesh	One node close to the center lying on the <i>X</i> -axis
X	Restrained	Free
Y	Free	Free
Z	Restrained	Restrained

Considering the abovementioned information, constant coefficients of friction between blank/punch and blank/die presented in [3] were assigned to the FE simulations. Coefficients of friction between blank/punch and blank/die are assumed to be 0.23 and 0.20, respectively.

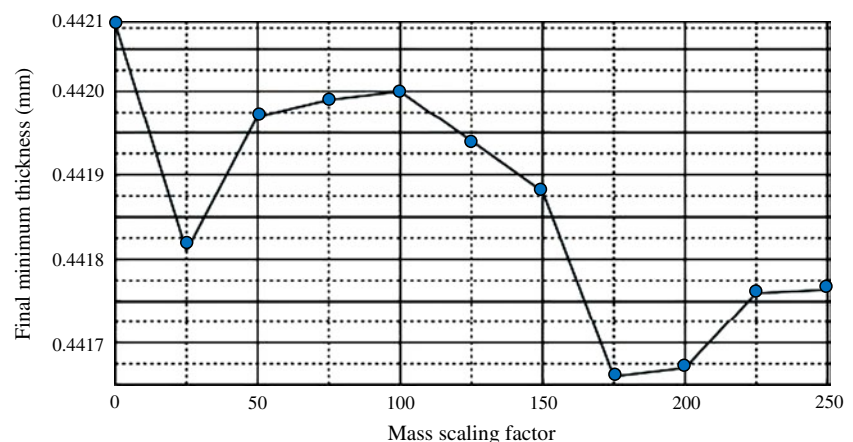
### 3 Experimental investigations

In the experiments, a hydraulic press with a maximum load capacity of 60 t and a constant punch speed of 6 mm/min was used. In this press, the punch and die were mounted, in turn, on the upper and lower shoes of the machine. The punch force and the punch stroke were measured separately by indicators that were provided on the machine. Figure 3 shows the hydraulic press employed in the experiments as well as the indicators.

In this study, a compressive force was applied to the sheet metal of diameter 120 mm by the blank holder and then punch moved down. Next, the thickness of the formed part was measured by a Cyclone Digitizer-series 2. The experimental results of the drawing of the aluminum sheet with diameter 120 mm are as follows: minimum thickness, maximum, and average punch forces are in turn, 0.433 mm, 8,750 N, and 4,960 N.

A blank of diameter 130 mm was also drawn into the die to investigate the accuracy of FE model for the prediction of fracture (BHF=2,174 N and punch displacement=24 mm).

**Fig. 4** Final STHs corresponding to different mass scaling factors



By applying the abovementioned conditions, fracture occurred when part thinning was more than 20 % (thickness was less than 80 % of initial thickness).

### 4 Finite element modeling

Much research based on the finite element analysis has been done to analyze the sheet metal forming processes. The accuracy and efficiency of FE analysis determine whether the simulation results are successful and reliable or not. One question being frequently asked is whether a model is valid or invalid [4]. This leads to research on model verification and model validation in this study.

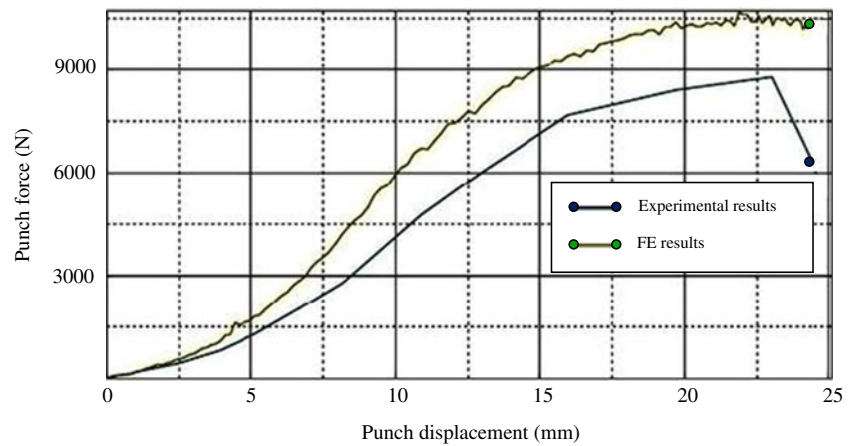
There are two types of FE codes, which can be used for sheet metal forming simulation, i.e., static codes and dynamic codes. Generally, without going into detail, both types of codes are based on equations of motion. It is reported in the literature [15] that there are some drawbacks in modeling of forming processes using static approach; accordingly, dynamic method is more efficient for the simulation of sheet metal-forming processes with high nonlinear nature.

In this research, the dynamic approach was employed and represented by ABAQUS/Explicit [16] to simulate the deep drawing process of a cup made from aluminum sheet. All the simulations performed in the current study were run on a Pro Mc 700 Laptop Computer and the FE results were validated by the experimental data.

#### 4.1 FE simulation parameters

This section describes some important features of the data and algorithms used in the simulation. In the FE simulation, the surfaces that define the shape of the tools were modeled as rigid bodies by using rigid elements available in ABAQUS/Explicit, i.e., four-node, bilinear quadrilaterals. The pure master-slave contact algorithm was utilized to simulate contact

**Fig. 5** Diagram of punch force–punch displacement in the drawing of aluminum 1100 with diameter 120 mm



between the rigid tools and the sheet material. The circular blank with 120 mm diameter and 0.49 mm thickness was modeled with 1,580 four-node, bilinear shell elements. In the case of ABAQUS/Explicit, the only available element is coded S4R. It is a thick shell element allowing for first-order transverse shear deformation [17]. Since the S4R element makes use of reduced integration, it is a uniform strain element. To avoid excitation of hourglass modes, which can lead to severe mesh distortion, a visco-elastic hourglass control was used. Boundary conditions applied to the sheet metal mesh are presented in Table 3.

In this simulation, the material was defined using an elastic–plastic model with in-plane anisotropy and this feature was described by Hill’s yield criterion. Anisotropy parameters F, G, H, L, M, and N were considered as stress ratios in ABAQUS/Explicit and determined based on Lankford’s coefficients  $r_0$ ,  $r_{45}$ , and  $r_{90}$  given in Table 2 [17]. By few assumptions, the constants F, G, H, and even N can be evaluated from simple tension tests; whereas shear tests are necessary to evaluate L and M for sheet metals. However, the determination of these parameters is not necessary since  $\gamma_{yz}$  and  $\gamma_{zx}$  are normally zero in sheet-forming processes.

The ABAQUS/Explicit time integration procedure requires very small time increments. For quasistatic problems, this may lead to extreme computation times. There are two common ways to cope with this problem, the increased speed of the

process and/or increased material density [17]. In the current analysis, the second method was employed.

It is known that as the mass scaling increases, the solution time decreases. Furthermore, the quality of the results also decreases but there is usually some level of scaling that improves the solution time without sacrificing the quality of the results.

One of the results of interest in this analysis is the final minimum thickness of the formed part, STH. Here, we can compare the results from each of the scaled analyses with the unscaled analysis results. Figure 4 shows final STHs corresponding to different mass scaling factors. As the figure demonstrates, the mass scaling case using a factor of 100 yields results that are not significantly affected by this factor. By the comparison of kinetic and internal energy histories, it was discovered that the kinetic-to-internal energy ratio is quiet low and consequently, no strong dynamic effect is induced in the model. In this FE simulation, the punch diameter, die diameter, fillet radius of punch/die, as well as blank diameter are set as 65, 70, 5, and 120 mm, respectively.

#### 4.2 Verification of FE model

By the application of blank holder force and punch displacement in  $Y$  direction and implementing the experimental conditions in FE simulation, some data were obtained. In this

**Fig. 6** Deep drawn parts in FE simulation and experiment

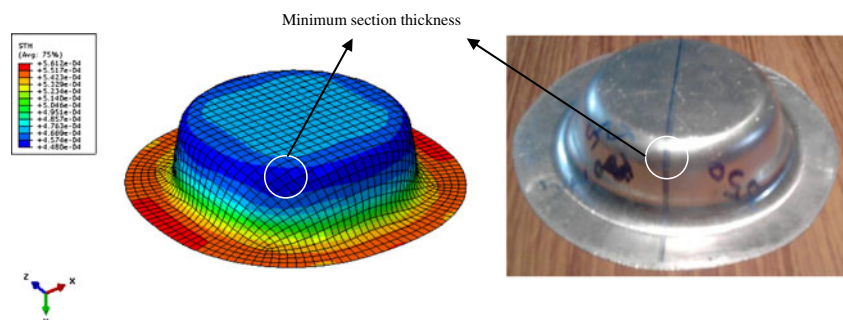
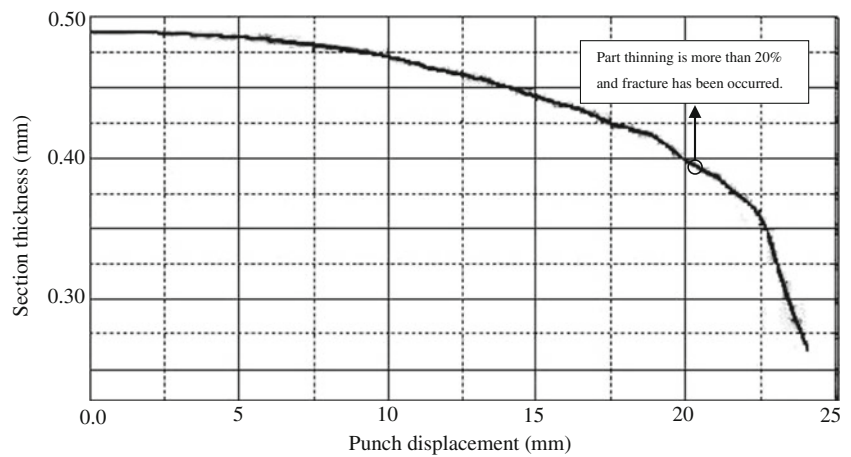


**Fig. 7** History output for section thickness in aluminum 1100 with diameter 130 mm (element 775)



simulation, minimum thickness, maximum and average punch forces were, in turn, determined as 0.4420 mm, 10,512 N, and 5,826 N. The diagram of punch force–punch displacement for the blank of 120 mm diameter is shown in Fig. 5. Figure 6 shows the deep drawn parts in FE simulation and the experiment. The detected error in final minimum thickness between FE simulation and experiment for the blank of 120 mm diameter was determined as 9 %. As stated in the former section, the material was defined using an elastic–plastic model with in-plane anisotropy and this feature was described by Hill’s yield criterion. It has been established that Hill’s criterion overpredicts the yield behavior of aluminum, especially, when the Lankford’s coefficients are less than unity. Although the results obtained from the tests revealed acceptable agreements with FE predictions of the final minimum thickness and punch force curve, there are some partial differences between the results. By more considerations of FE and experimental results, it is obvious that the FE model predicts the results more than those obtained by the experimental procedures and it can be concluded that the partial differences between FE and experimental data are to some extent natural.

Another important factor for the assessment of FE model is to determine the accuracy of the model from the perspective of fracture prediction. There are numerous methods in the literature [3, 6] to predict the fracture of sheet blank; however, maximum thinning in the part is commonly used in industry to indicate the probability of fracture. In the present study,

maximum thinning as a fracture criterion was employed, i.e., a maximum thinning of 20 % was used as the critical fracture criterion.

In order to verify the FE model from the perspective of fracture prediction, a sheet blank of 130 mm diameter was drawn into the die. In this simulation, the maximum thinning occurred in element 775. The output history of section thickness, STH, for this element is shown in Fig. 7. As can be seen in this figure, the part was torn by 20.605 mm punch displacement.

Figure 8 illustrates deep drawn parts in FE simulation and experiment. The detected error for the prediction of fracture between FE simulation and experiment for the blank of 130 mm diameter was determined as 8 %.

After the validation of FE results by experimental data, the rest of the tests were carried out by means of ABAQUS finite element package and considered as trusted data for the determination of local and global optimized BHG profiles.

## 5 Results and discussion

### 5.1 Stress analysis in the formed part

As aforementioned, in most conventional deep drawing processes, the blank holder force applied to the sheet blank is constant over punch stroke, whereas the state of stress in the

**Fig. 8** Deep drawn parts in FE simulation and experiment

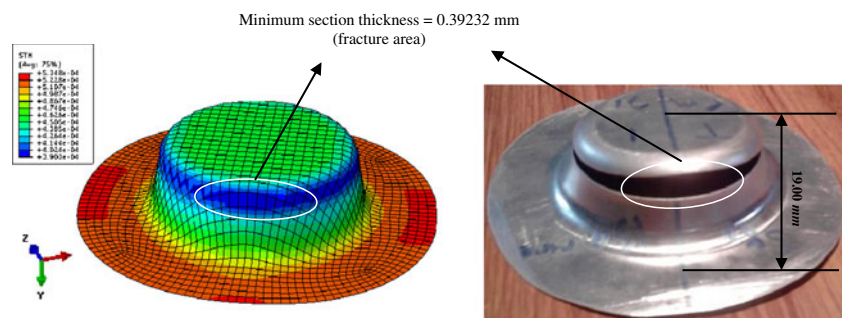
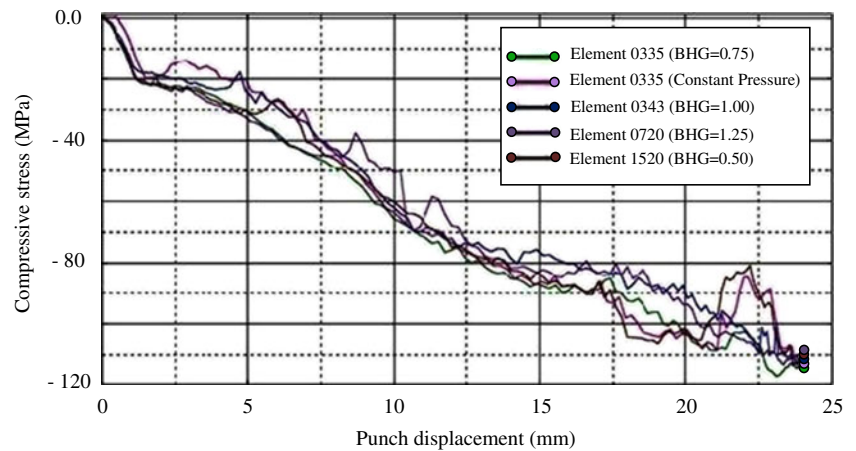


**Fig. 9** Compressive stresses of critical elements on the flange area



deforming material changes significantly. As a consequence, the process conditions that produce wrinkling and fracture also change. Since the state of stress in the deforming material changes noticeably, it is wise to change the blank holder force during deep drawing process. Variable BHF systems are designed based on this concept.

In deep drawing operation, wrinkling normally occurs at the flange and is generated by excessive compressive stresses that cause the sheet to buckle locally. It is known that the blank holder force must be increased in order to suppress the wrinkling growth and by this operation, the compressive stresses on the flange area can be desirably controlled. On the other hand, fracture or necking occurs in a drawn part which is under excessive tensile stresses. Under such conditions, it is reasonable to decrease blank holder force to allow the material flows into the die cavity. In modern stamping operations, BHF is not constant over the punch stroke and it is adjusted considering the state of stress in deforming material.

In deep drawing processes based on blank holder gap system, the mechanism of BHF adjustment is thoroughly

different and these systems operate according to the reaction force of blank holder to the sheet blank. In such systems, the reaction force applied to the sheet blank from blank holder is variable though the BHG is constant during the process.

In the beginning of deep drawing operation, the sheet blank is completely free and no restraining force is applied. By the movement of punch into the die cavity, the compressive stresses on the flange area are initiated and the wrinkles occur. As the punch penetrates into the die cavity, compressive stresses on the flange area increase and hereupon, the wrinkles grow as long as they get tangent to holder surface.

When the wrinkles are tangent to the holder surface and punch continues its movement, compressive stresses on the flange are intended to raise, i.e., the amplitude of wrinkles is being increased, whereas the holder surface prevents from wrinkling growth.

According to Newton's third law, the mutual forces of action and reaction between two bodies are equal, opposite, and collinear. In other words, the more wrinkles force the blank holder, the same amount of force is applied to the

**Fig. 10** Tensile stresses of critical elements on the sidewall

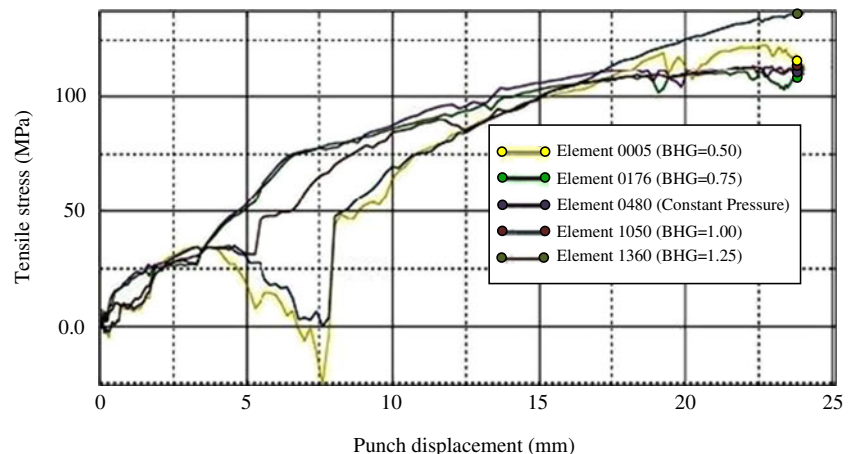
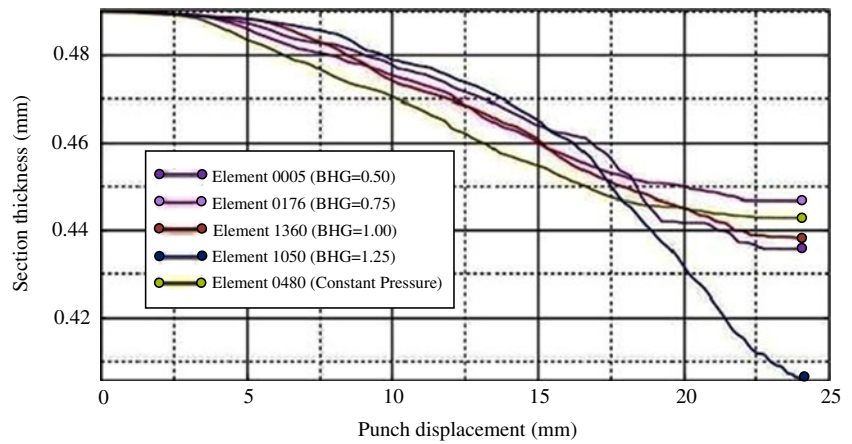


**Fig. 11** Histories of thinning in critical elements



wrinkles from the holder surface and it prevents wrinkles from excessive growth. Therefore, the reaction force applied to the sheet blank will be variable during the process though the BHG is constant over the punch stroke. Figure 9 shows the compressive stresses of critical elements on the flange area in the cases of constant BHF and constant BHGs ranging from 0.50 to 1.25 mm. As can be seen in this figure, hoop stress in the case of constant BHG 0.75 mm is more than the other cases and it leads to the prevention of excessive tensile stress in the sidewall as well as excessive thinning. Although the hoop stress in this case is more than the other samples, the magnitude of maximum compressive stress is in the allowable range. This is because wrinkling amplitude is controlled in the desired range.

Tensile stresses of critical elements on the sidewalls of the parts formed by constant BHF and constant BHGs ranging from 0.50 to 1.25 mm are shown in Fig. 10. Moreover, the histories of thinning in these critical elements are shown in Fig. 11. Considering these figures, it is clear that tensile stress and thinning in the case of constant BHG 0.75 mm are more desirably controlled in comparison with the other cases.

As aforementioned, the reacted blank holder force applied to the sheet blank is variable in BHG systems; however, the variation amplitude of this force is constant during the process. In this study, a novel approach is devised in order to change the variation amplitude of reacted BHF in deep drawing operation.

### 5.2 The concept of blank holder gap profile

In the previous researches, the BHG was constant over the punch stroke, i.e., the variation amplitude of reacted BHF was constant during the process. In the current study, however, BHG changes during the drawing operation which can affect the process conditions notably. Here, the variation of BHG over punch stroke is defined as BHG profile. One of the most important differences between this method and the other variable blank holder systems is to determine the desired BHG in

each punch step and consequently, it can improve the thickness of the drawn part.

In this study, six steps (punch displacement in each step was taken as 4 mm) were considered for punch stroke and in each step, a desirable blank holder gap among four different BHGs (0.50, 0.75, 1.00, and 1.25 mm) was determined (In the next part, it will be explained that why six punch steps were taken for BHG profile system). A sample blank holder gap profile is illustrated in Fig. 12.

By the comparison of different BHG profiles, the significant influence of this method on the thickness of formed part was revealed. Table 4 shows the final minimum thicknesses corresponding to different BHG profiles.

### 5.3 Optimization procedure

In many practical situations, one needs to set the process parameters in such a way that a desired output is obtained (in this case, the final minimum thickness is output parameter). This section shows that a properly selected blank holder gap profile can improve the thickness of formed part and result in the drawing of deeper parts.

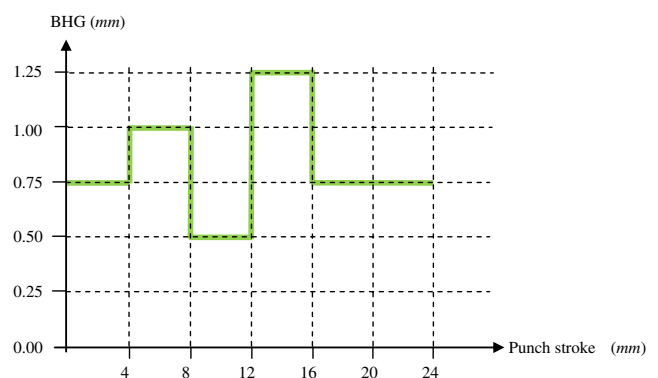


**Fig. 12** Sample blank holder gap profile

**Table 4** Final minimum thicknesses corresponding to different BHG profiles

Row	BHG -1 (mm)	BHG-2 (mm)	BHG-3 (mm)	BHG-4 (mm)	BHG-5 (mm)	BHG-6 (mm)	Final Minimum Thickness (mm)
1	1.00	1.00	1.00	0.75	1.25	1.25	0.392000 (plate is torn)
2	0.50	1.25	0.75	1.25	0.75	1.25	0.421277
3	0.75	1.00	0.75	0.75	0.75	0.75	0.445019

5.3.1 Local optimization method

In this method, the best BHG in each punch step is determined and then, local optimized BHG profile is achieved. The method is based on the selection of corresponding BHG to the best thickness of the formed part. In other words, in each punch step (4 mm displacement in Y direction) four FE simulations with different BHGs were performed and BHG corresponds to the desirable thickness was chosen as the best BHG. By applying the local optimization method, the optimum BHG profile was obtained. Table 5 shows different BHGs and corresponding thicknesses in each punch step. The improvement of final minimum thickness in comparison with constant blank holder force method is 6.13 %.

In this research, an analysis is carried out in order to investigate the sensitivity of BHG profile system to the number of punch steps. Figure 13 demonstrates final minimum thicknesses of the formed parts versus the number of punch steps in BHG profile system. As the figure shows, the best final minimum thickness is achieved using six-punch steps during the deep drawing process.

Although the process conditions were improved using local optimization method, there is still a serious problem in this optimization procedure. As aforementioned, an optimal BHG is determined in the first step and the second stage is simulated based on the optimum result of the first step and it is obvious that a localized effect in a particular stage can have successive effects in further simulations. Hence, devising a global approach for the determination of optimized BHG profile is of great importance. To resolve the massive problem mentioned for local optimization method, a new optimization procedure is proposed using design of experiments, artificial neural networks, and simulated annealing algorithm.

**Table 5** Different BHGs and corresponding section thicknesses

	STH in BHG-1 (mm)	STH in BHG-2 (mm)	STH in BHG-3 (mm)	STH in BHG-4 (mm)	STH in BHG-5 (mm)	STH in BHG-6 (mm)
BHG=0.50 (mm)	0.483406	0.474606	0.463658	0.453989	0.445068	0.392000
BHG=0.75 (mm)	0.484093	<b>0.477864</b>	<b>0.468097</b>	<b>0.459602</b>	<b>0.452122</b>	<b>0.448010</b>
BHG=1.00 (mm)	<b>0.484214</b>	0.475742	0.461676	0.448293	0.420087	0.435047
BHG=1.25 (mm)	0.484162	0.475717	0.46144	0.439359	0.431103	0.411998

5.3.2 Global optimization method

In this method, the best BHG profile was directly determined using artificial neural network and simulated annealing algorithm. At the first step, the empirical model for the prediction of final minimum thickness in terms of BHG profile was achieved by means of design of experiments and neural networks. In the next stage, the proposed model was implanted into a SA optimization procedure to identify a proper BHG profile that can produce the desired final minimum thickness.

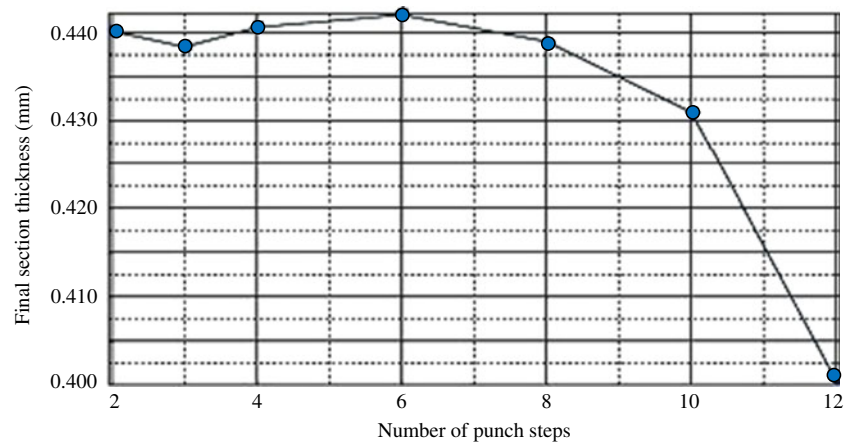
- (a) Modeling development using design of experiments (DOE) and ANN

In order to relate the blank holder gap profile to final minimum thickness, the BHG in each step was considered as process parameter, i.e., input parameter, and the final minimum thickness was chosen as the main process response characteristics. Accordingly, six process parameters, i.e., BHGs in different steps, were determined and the range of variation for each parameter was specified between 0.50 and 1.25 mm. The empirical model for the prediction of final minimum thickness in terms of the controlling parameters was established by means of neural networks. Since the FE model was validated by the experiments, the FE results could be treated as experimental data. Hence, the FE results were used to relate the BHG profile to final minimum section thickness.

The finite element results were obtained using DOE technique. Table 6 shows some of the finite element simulations settings obtained by D-optimal method. As shown, a total of 154 finite element simulations were performed to gather the required data. In this table, the first six columns show the process parameters settings given by D-optimal matrix. The last column is the measured output resulted from different finite element simulations.

In this study, the blank holder gap profile was modeled by a back propagation, multilayered neural network with an iterative learning method. Then, process parameters, i.e., different BHGs during the punch stroke or BHG profile, were optimized through SA algorithm. The FE dataset was divided into two sets as training and test sets. Neural networks make use of training dataset and test dataset to train the networks and

**Fig. 13** Final minimum thicknesses of the formed parts versus the number of punch steps in BHG profile system



evaluate their generalization capacity, respectively. The training data never used in test data. In this research, simulations were repeated many times with the different weight and bias initializations. After the investigation of various network training functions, it was discovered that TRAINLM can release the best results. TRAINLM is a network training function that updates weight and bias states according to Levenberg–Marquardt optimization [18]. Moreover, it is often the fastest backpropagation algorithm in the toolbox and is highly recommended as a first choice supervised algorithm [18]. Here, the final minimum thickness of formed part was

predicted with a backward multilayered neural network by using process parameters, BHG profile, as inputs to neural network (see Fig. 14). This neural network was trained with 126 datasets (BHG profiles). It was tested on 28 datasets, which were randomly chosen from different BHG profiles from the dataset, consists of 154 datasets.

The number of neurons used in the hidden layer of a neural network is extremely crucial in order to avoid overfitting problem, which hinders the generalization capability of the neural network. Number of neurons in hidden layers is usually determined with the trial-and-error approach [19, 20]. In this study, artificial neural networks with two, three, and four hidden layers were tested and 15 neurons were utilized in each layer as well. By considering various network structures and observing maximum and mean errors, the network structure 6-2-5-1 was chosen.

**Table 6** Finite element simulations settings obtained by D-optimal technique

Run	BHG-1 (mm)	BHG-2 (mm)	BHG-3 (mm)	BHG-4 (mm)	BHG-5 (mm)	BHG-6 (mm)	Minimum STH (mm)
1	1.00	0.75	0.50	0.50	1.25	1.25	0.437463
2	1.25	0.50	1.00	0.50	0.75	1.00	0.435728
...	...	...	...	...	...	...	...
10	1.00	1.00	1.25	0.75	0.50	0.50	0.392000
...	...	...	...	...	...	...	...
50	1.00	1.00	1.25	1.25	1.25	0.75	0.392000
51	0.50	1.00	0.75	1.25	0.50	0.75	0.41442
...	...	...	...	...	...	...	...
59	0.75	1.00	0.75	0.75	0.75	0.75	0.445019
...	...	...	...	...	...	...	...
100	1.00	1.25	1.25	1.25	1.00	0.75	0.408166
101	0.75	0.50	1.25	0.75	1.25	1.25	0.392000
...	...	...	...	...	...	...	...
109	1.00	0.75	1.00	0.75	0.75	0.75	0.442057
...	...	...	...	...	...	...	...
150	1.00	1.25	0.50	0.75	0.50	1.25	0.432947
151	1.00	1.00	0.50	1.00	0.75	1.00	0.438199
...	...	...	...	...	...	...	...
154	1.00	1.00	1.00	1.00	0.50	0.75	0.422478

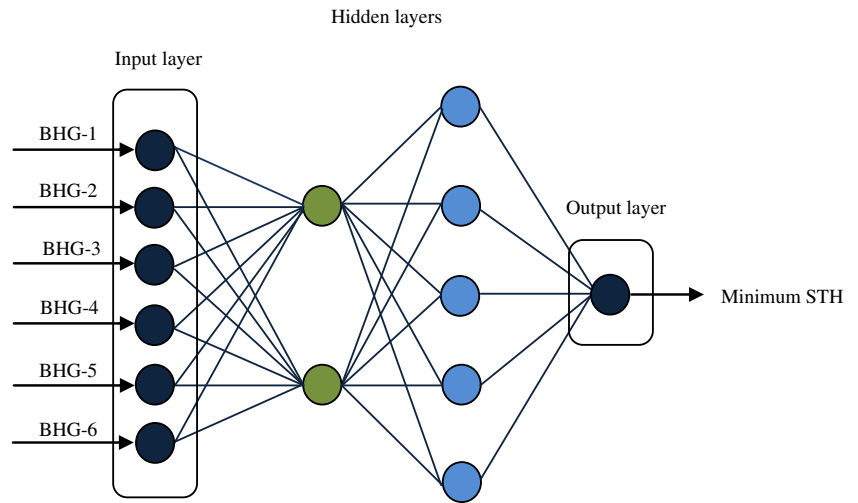
Table 7 shows prediction of some test dataset by the network, measured values, and calculated errors. The small errors of the test data confirm the reliability of this approach and it is observed that the computational neural network model provides high accuracy in predicting performance measure, i.e., final minimum thickness.

(b) Simulated annealing method

As mentioned above, determination of process parameters in such a way that a desired output is obtained is of utmost importance. Since finding the optimal set of input parameters for a given thickness is a massive problem, evolutionary algorithms can be employed as the optimizing procedure. The evolutionary algorithms are powerful optimization techniques widely used for solving combinatorial problems [21]. As a promising approach, one of these algorithms called SA is implemented for optimization purposes in this study.

The name and inspiration come from annealing in metallurgy, a technique involving heating and controlled cooling of a material to increase the size of its crystals and reduce their defects [22, 23].

**Fig. 14** Backward multilayered neural network



The SA code employed in this paper operates based on a neighborhood structure where at each step, the coded candidate solution is replaced by one of the neighbor combinations. In multivariable problems, such as the one investigated here, one of the variables is randomly selected. Then, a neighborhood is generated and its suitability for the next move is evaluated. If this new candidate exhibits higher objective function, i.e., better final minimum thickness, the move is accepted. Otherwise, another chance is given to this move as it helps escaping the local optimum point.

In this study, a range of variation was assigned for the design variables, i.e., process parameters. These parameters (BHG in different steps) were discretized according to practical limitations by the steps of 0.05 mm. After the optimization process by the aid of SA algorithm, the global optimum BHG profile (0.50, 0.50, 0.50, 0.50, 0.75, and 0.75) was

proposed. Final minimum thickness of the drawn part using this set of BHGs was 0.44321 mm predicted by neural network and 0.44980 mm calculated by finite element simulation. By the comparison of minimum thicknesses in the parts formed by the global optimum BHG profile and constant blank holder force method, the improvement of thickness by 8 % was obtained. Figure 15 shows the flowchart of local and global optimization processes. As can be seen in this figure, the range of BHG variation was determined between  $t_0$  and  $2t_0$  since local and global optimized BHG profiles were restricted between these two extents.

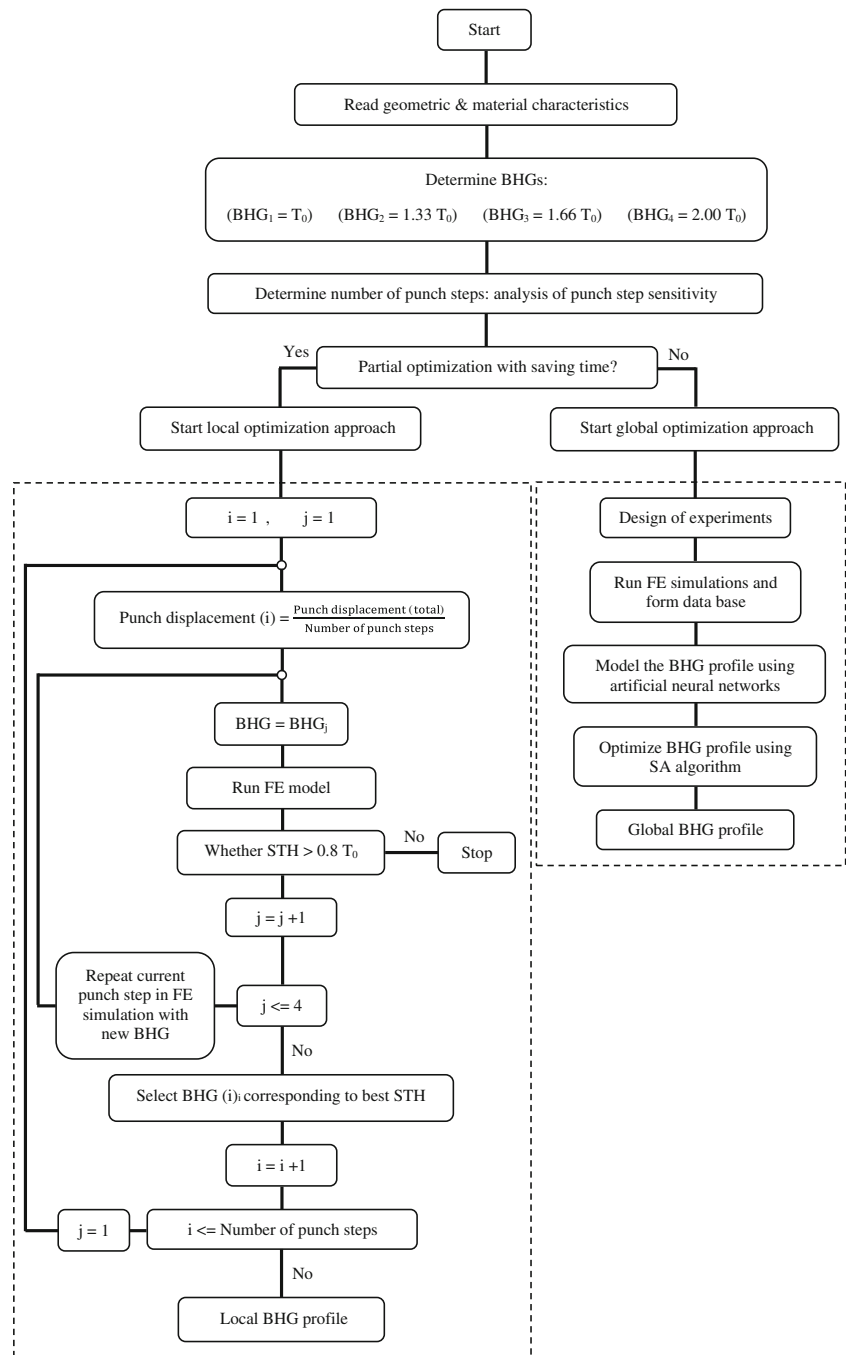
#### 5.4 Generalization of BHG profile approach

In previous sections, the concept of BHG profile, i.e., variation of BHG over punch stroke was introduced and it was

**Table 7** Prediction of test dataset by the network, measured values, and calculated errors

Row	BHG-1 (mm)	BHG-2 (mm)	BHG-3 (mm)	BHG-4 (mm)	BHG-5 (mm)	BHG-6 (mm)	Measured value (mm)	Predicted by NN (mm)	Error
1	1.00	0.50	0.50	1.00	1.00	0.50	0.420809	0.406524	0.033946
2	1.00	1.00	1.25	0.75	0.50	0.50	0.39200	0.393829	0.004666
3	0.75	1.25	0.50	1.25	1.25	1.25	0.39200	0.389049	0.007528
...	...	...	...	...	...	...	...	...	...
9	1.00	0.50	0.75	0.75	0.75	1.25	0.442174	0.435824	0.014361
10	1.00	1.00	1.25	1.25	1.25	0.75	0.39200	0.389049	0.007528
...	...	...	...	...	...	...	...	...	...
18	1.25	1.25	1.00	1.00	0.50	1.00	0.416928	0.416871	0.000137
19	1.25	0.75	0.75	0.75	1.25	0.75	0.39200	0.399388	0.018847
20	1.00	1.25	1.25	1.25	1.00	0.75	0.408166	0.394922	0.032447
...	...	...	...	...	...	...	...	...	...
26	1.00	0.50	1.00	1.25	0.75	0.75	0.427419	0.430987	0.008347
27	0.50	1.00	0.75	0.75	0.50	1.25	0.430183	0.417015	0.030609
28	0.75	0.50	0.50	0.50	1.25	0.50	0.432594	0.426404	0.014309

**Fig. 15** Flowchart of local and global optimization processes



shown that a properly selected BHG profile can improve the section thickness of formed part and result in the drawing of deeper parts. Thenceforth, two methods were devised for the optimization of BHG profile, i.e., the local and the global optimization methods. Although the approach employed in this research improved the thickness distribution of formed parts, there are still some issues which can be taken into account in order to promote robustness of the method.

In view of the abovementioned discussions, the first issue which may overwhelm the researchers is if the concept of BHG profile can be generalized into various materials,

thicknesses and diameters, or not. Consequently, investigating the effectiveness of BHG profile method in a variety of blank thicknesses, diameters, and materials can create a great deal of excitement among the researches. However, it should be noted that the material and geometric characteristics cannot be taken into account as state variables in BHG profile approach since the number of input parameters will be beyond the control and it reduces the effectiveness of the method. Hence, it is wise to apply the concept of BHG profile to various geometric characteristics and materials in order to explore the robustness of the approach.

**Table 8** Chemical composition and mechanical properties of SUS 304

Nuance	C %	Mn %	P %	S %	Si %	Cr %	Ni %	N %	$\sigma_y$ MPa	$\sigma_{UTS}$ MPa	Young's module GPa
SUS 304	0.08	2	0.045	0.03	0.75	18–20	8–10.50	0.10	265	573	191.7

In this paper, two methods were proposed in order to optimize BHGs over punch stroke, i.e., local and global optimization methods. It is evident that global optimization approach dominates all possible BHG profiles and if local BHG profile method improves section thickness of the formed part, global BHG profile approach will definitely ameliorate thickness distribution (at least as a same amount of local BHG profile). In this section, therefore, local optimization approach will be applied (due to saving time) to a variety of initial thicknesses, blank diameters, and materials in order to examine the robustness of approach.

#### 5.4.1 Material properties of sheet blanks

In the current research, the concept of BHG profile was examined into sheet blanks of aluminum 1100 and superiority of the approach in comparison with constant BHG/BHF methods was approved; whereas investigating this optimization approach in other materials such as stainless steel 304 (SUS 304) can also extend beyond this method. The chemical composition and mechanical properties of the material used in this section are presented in Table 8. Similar to aluminum alloy 1100, a complete experimental characterization was carried out in order to identify the material behavior. Here, all tensile tests were performed at 0°, 45°, and 90° to the RD for the investigation of sheet metal anisotropy. Logarithmic strain and stress were used to plot stress–strain data (see Fig. 16).

In this section, firstly, an analysis was performed in order to investigate the sensitivity of BHG profile system to the

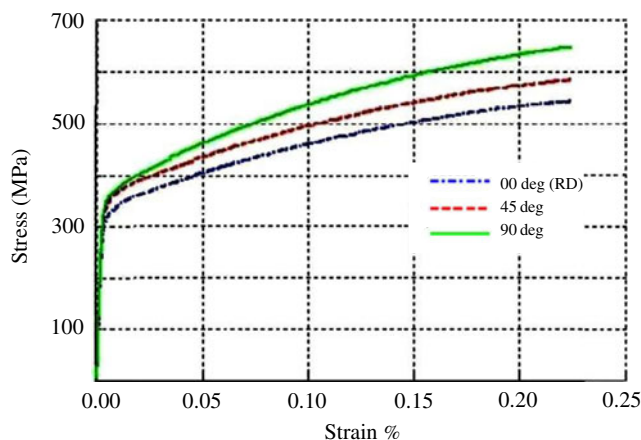


**Fig. 16** Stress–strain curves at different degrees to the rolling direction (SUS 304)

number of punch steps in SUS 304. Figure 17 demonstrates the final minimum thicknesses of formed parts versus the number of punch steps in BHG profile system (initial thickness=0.50 mm and blank diameter=120 mm).

As the figure shows, the best final minimum thickness was achieved using four-punch steps during the deep drawing process. Then, the element which had maximum thinning was identified and the output history of section thickness for this element was compared with that obtained from constant BHF system (see Fig. 18).

As the figure illustrates, thinning is more favorably controlled by using BHG profile approach and it can be concluded that this method can offer a broad range of benefits in other materials such as steel alloys. By the comparison of minimum thicknesses in the parts formed by local optimum BHG profile and constant blank holder force method, the improvement of thickness by 10.03 % was obtained and efficacy of this approach in steel alloys was also approved. As reported, the amount of thickness improvement in steel alloys is more than that of aluminum alloy 1100 by the application of BHG profile method. One of the most important reasons for this behavior is that the thinning rate in aluminum alloy 1100 is more than that of stainless steel 304 in the same process conditions and it can reduce the effectiveness of optimization processes, in particular, BHG profile approach. Figure 19 shows the section thickness of critical elements versus punch displacement in Al 1100 and SUS 304 (initial thickness of the sheet blanks=0.50 mm, blank diameters=120 mm).

#### 5.4.2 Geometry of sheet blanks

In stamping operation, the initial thickness and diameter of sheet blanks play indispensable roles in determining the failure of a product and accordingly, application of BHG profile approach to sheet blanks with a variety of initial thicknesses and diameters to inspect robustness of this approach can be actually arousing. In this section, BHG profile method is applied to sheet blanks of Al 1100 and SUS 304 with various thicknesses and diameters and then, effectiveness of the approach will be investigated. The amounts of thickness improvement in the drawn parts of Al 1100 and SUS 304 versus blank geometry are schematically shown in Figs. 20 and 21.

In view of these figures, dependency of BHG profile approach to blank diameter is to some extent visible and sheet blanks of greater diameters can be partially influenced by this method. It is likely that the less efficiency of the approach in sheet blanks of greater diameters can be related to the amount

**Fig. 17** Final minimum thicknesses of the formed parts versus the number of punch steps in BHG profile system (SUS 304)

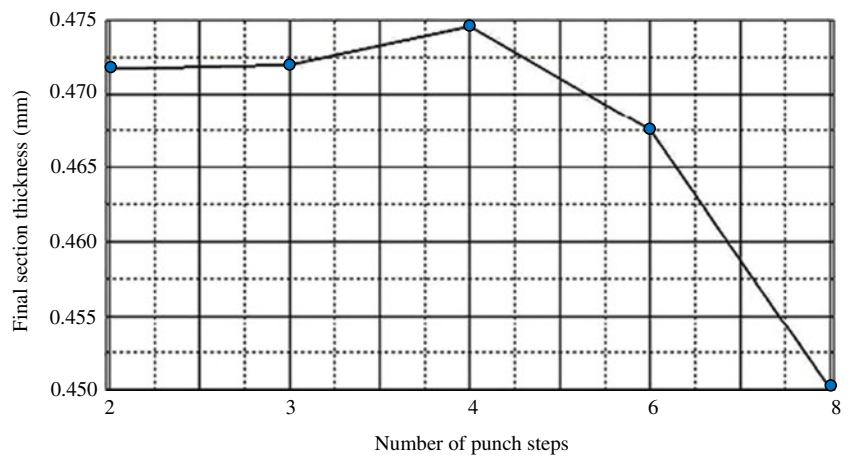
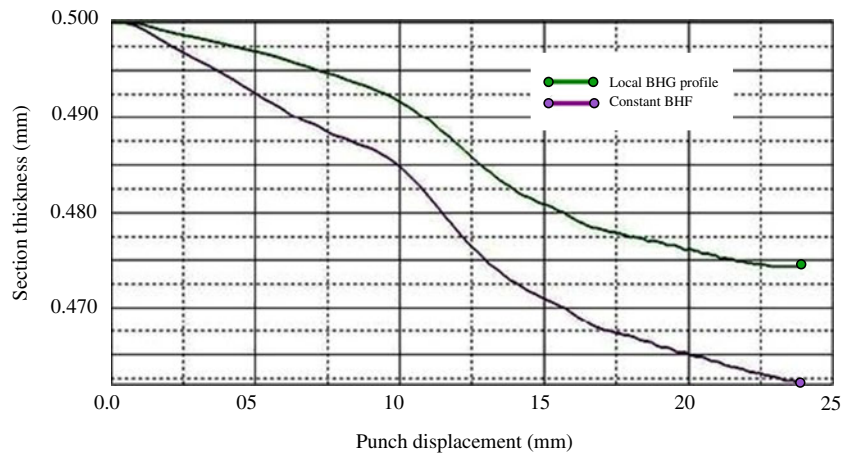


**Fig. 18** History output for section thickness in critical elements (SUS 304)



of material flow into the die cavity. It is reported in the literature that the material flow of sheet blanks is reduced by increasing the blank diameters and it can increase the thinning rate of the formed parts. Consequently, the efficiency of BHG profile method is expected to be decreased. Figures 22 and 23

illustrate the history output of section thickness in the critical elements versus punch displacement for blanks of thicknesses 1.00 mm with various diameters (two samples). As can be seen in this figure, thinning rates are raised by increasing the blank diameter.

**Fig. 19** History output for section thickness in critical elements (SUS 304 and Al 1100)

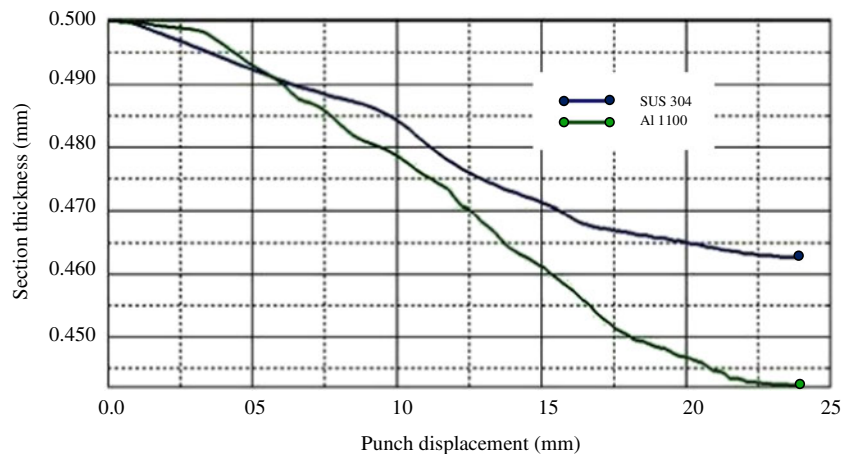


**Fig. 20** Thickness improvement in the drawn parts of Al 1100 versus blank geometry

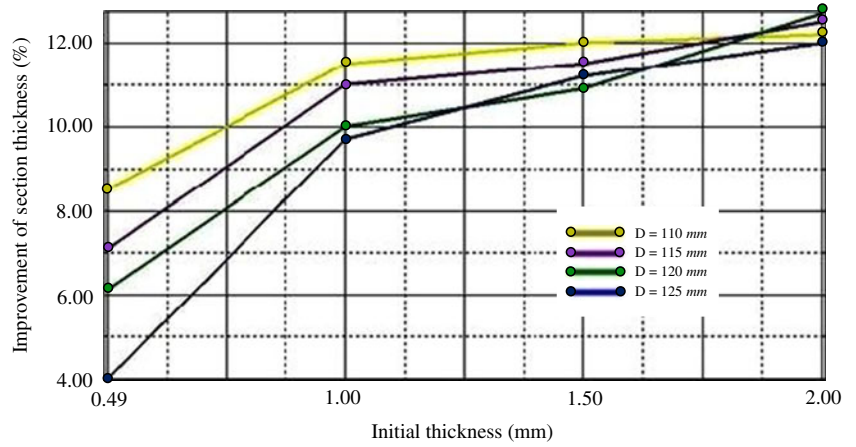
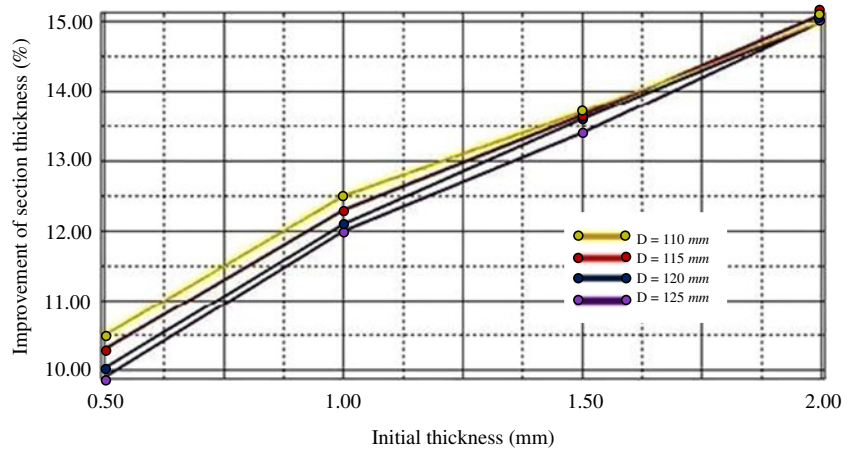


**Fig. 21** Thickness improvement in the drawn parts of SUS 304 versus blank geometry



Furthermore, the efficacy of BHG profile approach in improving the thickness distribution of the formed parts (in both materials) is raised by increasing initial thickness of sheet blanks. The main cause for this improvement is also related to different thinning rates in sheet blanks with various initial thicknesses. It was observed that as initial thicknesses of sheet

blanks increase, the thinning rates in the formed parts gradually decrease. The other reason for this behavior is the larger space of material deformation in the flange area; in other words, blank holder gap gets larger by increasing the initial thickness of the sheet blank since it is a percentage of the blank thickness.

**Fig. 22** History output of section thickness in critical elements for blanks of thicknesses 1 mm (Al 1100)

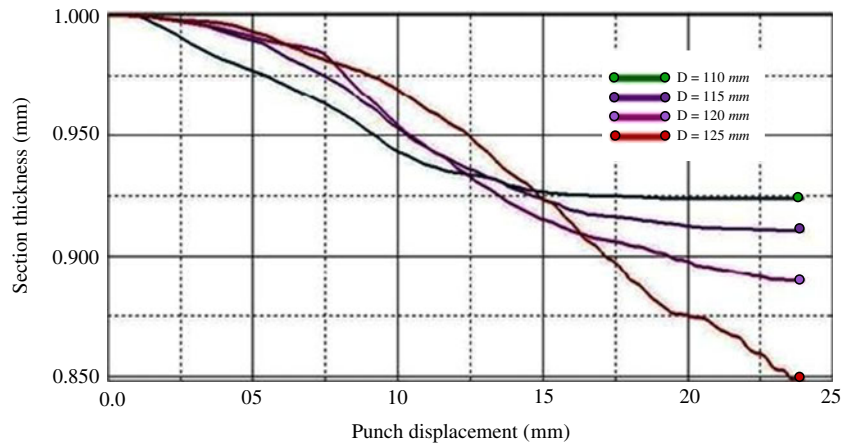
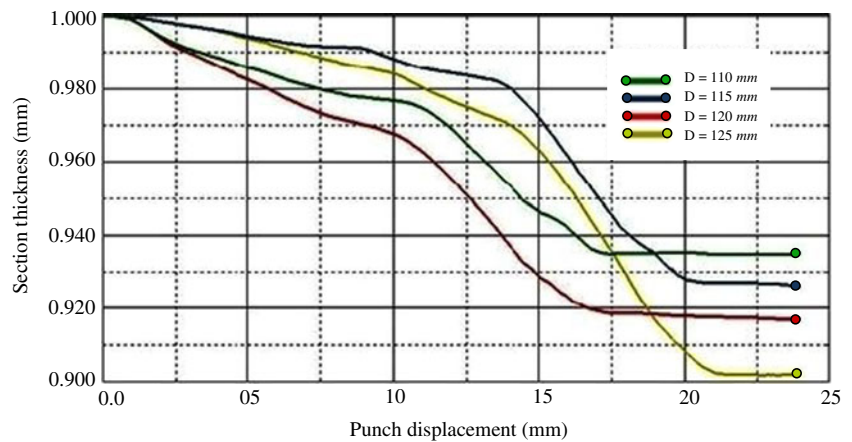


**Fig. 23** History output of section thickness in critical elements for blanks of thicknesses 1 mm (SUS 304)



### 6 Experimental verification of optimized BHG profiles

The aim of this section is to verify the feasibility of the process and validate the results gained by FE simulations. Hence, two experiments are performed to validate the local and global optimized BHG profiles in aluminum alloy Al 1100. In these tests, the punch stroke was divided into six steps, i.e., punch displacement in each step was 4 mm, and in each step, a suitable BHG was assigned. Four spacers and fixers were used to provide the required BHG in each step. In experimental investigations, final minimum thicknesses of the drawn parts of Al 1100 with initial blank diameter 120 mm were determined. STHs of drawn parts using local and global optimized BHG profiles are 0.439 and 0.442 mm, respectively. These results show the improvement of minimum thickness for both optimization methods. Afterward, a variety of experiments (32 verification tests) are conducted to examine the generalization of approach and the amounts of thickness improvement in the formed parts of Al 1100 and SUS 304 are identified. The experimental investigation has revealed acceptable agreements between FE and experimental results (see Figs. 24 and 25).

Some of the tests performed in this study with various initial thicknesses, blank diameters, and materials are presented in Table 9. It should be noted that in the experiments, wrinkles are suppressed after each punch step and then, the next step is performed.

### 7 Conclusions

In this paper, the concept of BHG profile, the variation of BHG over punch stroke, was introduced. The local and the global optimization methods were used in order to determine the optimized blank holder gap profile. The first method was based on the selection of corresponding BHG to the best section thickness of the formed part in each punch step. The second method, however, used neural networks and simulated annealing algorithm to find global optimized BHG profile. Although the process conditions were improved using local optimization method, there was still a serious problem in that optimization procedure. In local optimization method, an optimal BHG was determined in the first step and the second

**Fig. 24** Experimental results for thickness improvement in the drawn parts of Al 1100 versus blank geometry

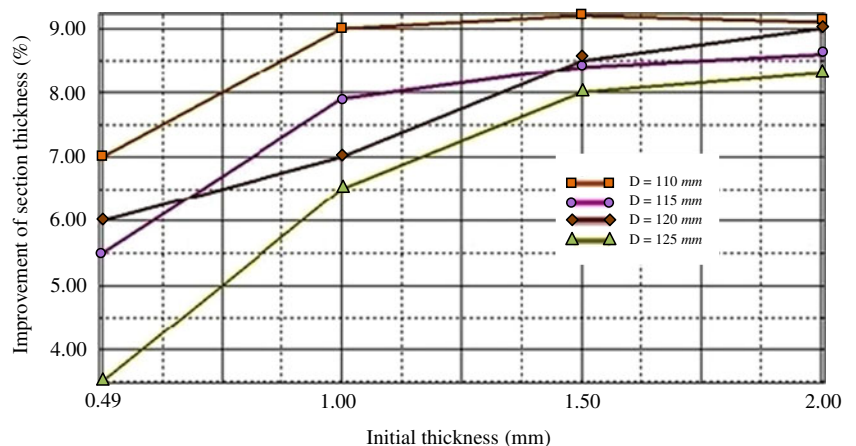
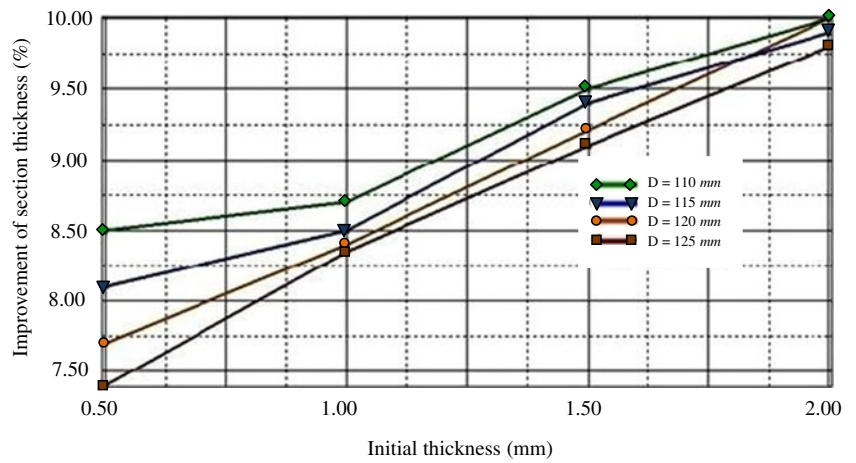


**Fig. 25** Experimental results for thickness improvement in the drawn parts of SUS 304 versus blank geometry



stage was simulated based on the optimum result of the first step and consequently, a localized effect in a particular stage had successive effects in further simulations. The global optimization procedure was proposed in order to resolve this massive drawback. In global optimization approach, all effective parameters in deep drawing process including the state of stress, loading history, and thinning were considered indirectly and then, the global optimized BHG profile was achieved.

Since this method examines all possible BHG profiles and then selects the best one, global optimization approach is superior to the local optimization method. Although the approaches employed in this research improved the thickness distribution of formed parts, there were still some issues which should be taken into account in order to promote robustness of the method. The most important issue was if the concept of BHG profile can be generalized into various materials,

**Table 9** Experimental results for the drawing of Al 1100 and SUS 304 with various geometric characteristics

Row	Material	Initial Thickness (mm)	Blank Diameter (mm)	Thickness Improvement (%)	Drawn Parts
1	Al 1100	0.49	125	3.50	
2	SUS 304	1.00	120	8.40	
3	Al 1100	1.50	115	8.40	
4	SUS 304	2.00	110	10.00	

thicknesses and diameters or not. To study this issue, the concept of BHG profile was applied to steel alloy SUS 304 and various geometric characteristics. Similar to aluminum alloy 1100, thinning was more favorably controlled by using BHG profile approach in comparison with constant BHF method and it was concluded that this method can offer a broad range of benefits in other materials such as steel alloys. Afterward, the proposed approach was applied to a variety of initial thicknesses and diameters of sheet blanks. It was reported that efficacy of BHG profile method in improving the thickness distribution of formed parts (in both materials) was raised by increasing initial thickness of sheet blanks. Moreover, dependency of BHG profile approach to blank diameter was to some extent visible and sheet blanks of greater diameters were partially influenced by this method. Finally, a variety of experiments were conducted in order to validate local and global optimized BHG profiles and examine the generalization of the proposed approach. The experimental investigation has revealed acceptable agreements between FE and experimental results. About the limitation of this method, it should be mentioned that deep drawing operation is usually performed using conventional hydraulic presses; whereas it is reasonable to employ a hydraulic press with computer numerical position control system to implement BHG profile approach. As a consequence, it can be considered as a limitation of this method.

**Acknowledgments** This work was supported by Ferdowsi University of Mashhad. Our collaboration with Dr. Kolahan's research group as well as Mr. Manoochehri is also gratefully acknowledged.

## References

- Cao J, Boyce MC (1997) A predictive tool for delaying wrinkling and tearing failures in sheet metal forming. *ASME J Eng Mater Technol* 119:354–365
- Yagami T, Manabe K, Yamauchi Y (2007) Effect of alternating blank-holder motion of drawing. *J Mater Process Technol* 188:187–191
- Sheng ZQ, Jiratheeranat S, Altan T (2004) Adaptive FEM simulation for prediction of variable blank-holder force. *Int J Mach Tools Manuf* 44:487–494
- Chen L, Yang JC, Zhang LW, Yuan SY (2007) Finite element simulation and model optimization of blank-holder gap and shell element type in the stamping of a washing-trough. *J Mater Process Technol* 182:637–643
- Huaibao W, Weili X, Zhongquin L, Yuying Y, Wang ZR (2002) Stamping and stamping simulation with a blank-holder gap. *J Mater Process Technol* 120:62–67
- Thomas W (1999) Product tool and process design methodology for deep drawing and stamping of sheet metal parts. Dissertation, Ohio State University
- Sibel E, Beisswanger H (1995) Deep drawing process. Carl Hanser, Munich
- Siegert K, Dannenmann E, Galeikoet A (1995) Closed loop control system for blank-holder forces in deep drawing. *Ann CIRP* 44(1):251–254
- Cao J, Boyce MC (1994) Design and control of forming parameters using finite element analysis. Symposium on Computational Material Modeling, Chicago
- Gavas M, Izciler M (2007) Effect of blank-holder gap on deep drawing of square cups. *Mater Des* 28:1641–1646
- Sing KS, Kumar RD (2004) Application of a neural network to predict thickness strains and finite element simulation of hydro-mechanical deep drawing. *Int J Adv Manuf Technol* 25:101–107
- Cao J, Kinsey B, Solla SA (2000) Consistent and minimal springback using a stepped binder force trajectory and neural network. *J Eng Mater-T ASME* 122:113–118
- Satoshi K, Kenta K, Koetsu Y (2011) Optimization of variable blank-holder force trajectory by sequential approximate optimization with RBF network. *Int J Adv Manuf Technol* 61:1067–1083
- Chamekh A, BenRhaïem S, Khaterchi H, BelHadjSalah H, Hambli R (2010) An optimization strategy based on a meta-model applied for the prediction of initial blank shape in a deep drawing process. *Int J Adv Manuf Technol* 50:93–100
- Kawaka M, Olejnik L, Rosochowski A, Sunaga H, Makinouchi A (2001) Simulation of wrinkling in sheet metal forming. *J Mater Process Technol* 109:283–289
- ABAQUS finite element package 6.10.1
- ABAQUS user's manual
- MATLAB user's manual
- Ozel T, Karpat Y (2005) Predictive modeling of surface roughness and tool wear in hard turning using regression and neural networks. *Int J Mach Tools Manuf* 45:467–479
- Tae JK, Kim HS (1998) Autonomous cutting parameter regulation using adaptive modeling and genetic algorithms. *Precis Eng* 22(4): 243–251
- Kolahan F, Khajavi H (2010) A statistical approach for predicting and optimizing depth of cut in AWJ machining for 6063-T6 Al alloy. *Int J Mech Syst Sci Eng* 5(2):143–146
- Venkataraman P (2002) Applied optimization with MATLAB programming. Wiley, New York
- Laarhoven PJ, Aarts EL (1987) Simulated annealing theory and applications. Kluwer, London